Arch Pharm Res Vol 33, No 5, 727-735, 2010
DOI 10.1007/s12272-010-0512-y

Archives of Pharmacal Research
www.springer.com/12272

Intratracheal Instillation of Platinum Nanoparticles May Induce Inflammatory Responses in Mice

Eun-Jung Park[1], Hero Kim[2], Younghun Kim[2], and Kwangsik Park[1]

[1]College of Pharmacy, Dongduk Women's University, Seoul 136-714, Korea and [2]Department of Chemical Engineering, Kwangwoon University, Seoul 139-701, Korea

(Received December 23, 2009/Revised February 26, 2010/Accepted March 1, 2010)

Platinum nanoparticles (PNPs) are potentially useful for sensing, catalysis, and other applications in the biological and medical sciences. However, toxicity data on the PNPs are very limited. In this study, we prepared PNPs using K_2PtCl_6, (21 nm in phosphate buffered saline) and tested inflammatory responses in mice after a single intratracheal instillation. The concentrations of pro-inflammatory cytokines (IL-1, TNF-α, and IL-6), TH0 cytokine (IL-2), TH1-type cytokine (IL-12), and TH2-type cytokines (IL-4 and IL-5) were increased in broncho-alveolar lavage fluid by PNPs. It was found that the induciton of TH2-type cytokines were higher than TH1-type cytokine on day 28 after instillation. TGF-β was also significantly increased in broncho-alveolar lavage fluid during the experimental period. IgE level in serum was increased with the increase of B cells distribution. Intracellular level of glutathione (GSH) was diminished by treatment of PNPs. When the distribution of T cell subtype ($CD4^+/CD8^+$) was analyzed, the ratio was decreased. Gene expression of matrix metalloproteinases was found to be significantly increased on day 1. By histopathological examination, cell infiltration of macrophages and neutrophils was observed in lung tissue during the experimental period. Based on these findings, it is suggested that the exposure to PNPs may induce inflammatory responses in mice.

Key words: Platinum nanoparticles, Intratracheal instillation, Inflammation, Cytokines

Selected by Editors

INTRODUCTION

Metal nanoparticles such as titanium, ceria, silver, and platinum have potentially useful applications in many industrial fields. Among these metal nanoparticles, platinum nanoparticles (PNPs) have been widely used as a catalyst due to their high conductance and reactivity. Enhancement of the selectivity in chemical reactions by PNPs has been a much-researched topic. For example, selective hydrogenation of *o*-chloronitrobenzene to *o*-chloroaniline has been performed using polyethylene glycol-stabilized PNP (Cheng et al., 2009). When different shapes and types of array catalysts were prepared using platinum particles and tested for oxygen reduction reaction, PNP showed a high sensitivity (Komanicky et al., 2009).

PNPs have also been proved to have a protective effect on reactive oxygen species. In previous reports, PNPs do not show cytotoxicity in several different cultured cells (TIG-1, MI-38, MRC-5, HeLa, and HepG2), although cellular uptake of PNPs does occur in a time- and dose-dependent manner (Hamasaki et al., 2008). PNPs have been shown to protect cells from oxidation-induced inflammation by scavenging superoxide anion ($O2^-$) and hydroxyl radical (·OH) in aqueous solution, and they inhibit pulmonary inflammation in mice exposed to cigarette smoke by preventing antioxidant depletion and inhibiting neutrophil infiltration and NF-κB activation (Onizawa et al., 2009). Due to these reasons, PNPs have been widely used in biological and medical sciences. For example, PNPs containing cobalt and yolk-shell nanocrystals of FePt@CoS2 are known

Correspondence to: Kwangsik Park, College of Pharmacy, Dongduk Women's University, Seoul 136-714, Korea
Tel: 82-2-940-4522, Fax: 82-2-940-4159
E-mail: kspark@dongduk.ac.kr

to be more potent than cisplatin in killing HeLa cells (Gao et al., 2008). PNPs in combination with multi-walled carbon nanotubes also increase the sensitivity of the electrochemical DNA biosensor (Wang et al., 2006).

However, some workers who have been exposed to platinum during the refining processes manifested inflammatory diseases such as rhinitis, conjunctivitis, and asthma. Inhalation is the most common route of allergen entry, and 'platinosis' is considered to be an allergic response to complex platinum salts. Furthermore, some researchers suggest that platinum induces damage to cells through oxidative stress and inflammatory signals (Theron et al., 2004; Schmid et al., 2007). Although this topic has prompted lively debate, very little information is available regarding the safety and potential hazards of manufactured PNPs.

In this study, we prepared PNP from K_2PtCl_6, and characterized physico-chemical parameters such as size distribution, shape, and surface charge. We also investigated the inflammatory responses in mice following the intratracheal instillation of PNPs to elucidate the discrepancy between toxicity and protective effect.

MATERIALS AND METHODS

Preparation of PNPs

A mixture of 3 mL of 6 mM K_2PtCl_6 aqueous solution, x mL of double-distilled water, and y mL of alcohol (x+y= 197 mL) containing 100 mg of polyvinylpyrrolidone (PVP) was refluxed in a 250 mL flask for 3 h in an air-conditioned environment until the ethanol evaporated. The resulting product in the water-phase showed black suspension. Finally, this suspension was diluted with PBS (2X, 0.15M, pH 7.2) for instillation to mice. Solvent vehicle for control mice was prepared by the same procedure without K_2PtCl_6 (Teranishi et al., 1999).

Particles size measurements in PBS were performed using a submicron particle sizer (NICOMP^{TM}), images of the nanoparticles were acquired by transmission electron microscopy (TEM; JEM1010, JEOL), and the surface charges of the nanoparticles were measured using the zeta potential analyzer (Brookhaven instruments corp.).

Animals

ICR male mice (25 ± 1 g, 6 week) were purchased from Orient-Bio Animal Company and were allowed to adapt to the conditions in the animal room prior to the beginning of the study. The environmental conditions were strictly controlled, with temperature of 23 ± 1°C, relative humidity of 55 ± 5%, and a 12 h light/dark cycle. Animals used in this study were cared for in accordance with the principles outlined in the "Guide for the Care and Use of Laboratory Animals" issued by the Animal Care and Use Committee of NVRQS (National Veterinary Research and Quarantine Service).

Intratracheal instillation and sample preparation

PNPs were delivered with a 24-gauge catheter in a single dose by intratracheal instillation under light tiletamine anesthesia. Mice were sacrificed at day 1, 7, 14, 28 after treatment (n=12 per each time point). Three test samples were prepared by pooling 4 sera or broncho-alveolar lavage (BAL) fluid for the respective time point. Blood was collected from the retro-orbital venous plexus into heparinized capillary tubes on day 1, 7, 14 and 28 after instillation. A portion (20 μL) of the whole blood samples was aliquot for cell phenotype analysis, and the rest was centrifuged at 13,000 rpm for 10 min to obtain a serum for cytokine assay. BAL fluid collection was performed by cannulating the trachea and lavaging the lungs with 1 mL of cold PBS. Approximately 500~600 μL BAL fluid was harvested per mouse and this was centrifuged at 3,000 rpm for 10 min. The supernatants were used to measure cytokines and the pellets were used to measure GSH.

To isolate the splenocytes, the spleen was aseptically removed from an ICR mouse and suspended by passage through a sterile plastic strainer in Dulbecco's Modified Eagle's Medium (DMEM) with 2% fetal bovine serum (FBS). After centrifugation at 1,500 rpm for 3 min, the supernatant was discarded and the pellet was briefly vortexed in 500 μL distilled water, then resuspended in DMEM with 2% FBS. The cells were filtered through a nylon mesh to yield the final splenocytes (Manosroi et al., 2005; Vendrame et al., 2006; Cho et al., 2007).

Measurement of GSH

The level of GSH was determined using ortho-phthaldialdehyde (Sigma-Aldrich) by substrate. We added 1% of perchloric acid to the cell pellet and left it on ice for 10 min. The cell lysates were centrifuged at 13,000 rpm for 5 min prior to analysis in order to remove precipitated protein. Cell lysates, KH_2PO_4/EDTA buffer, and o-phthaldialdehyde were placed in 96-black well plates and incubated at room temperature for 30 min. Fluorescence was measured using the microplate spectrofluorometer (GeminiXPS, Molecular Devices) with an excitation wavelength of 350 nm and an emission wavelength of 420 nm (Park et al., 2008). Results

were calculated as nmol of glutathione per mg of protein and presented as a percentage of the control group. The values were compared using the student's t-test, and levels of significance were represented for each result. Protein assays in the cell lysate were performed using BCA protein assay kit (Pierce, Rockfold).

Measurement of cytokines and IgE

The concentrations of each cytokine and IgE in serum and BAL fluid were determined using commercially available ELISA kits (eBioscience) and IgE ELISA kits (Komabiotech). The experiments were performed according to the protocol provided by the manufacturer. Finally, reactions were stopped by adding 1 M H_3PO_4 and 2N H_2SO_4, respectively, and the absorbance was measured at 450 nm using an ELISA reader (Molecular Devices). The amount of cytokine was calculated from the linear portion of the standard curve (Park et al., 2009).

Immunophenotyping

All monoclonal antibodies were purchased from eBioscience. T cells (CD3, 1:50), B cells (CD19, 1:50), NK cells (DX5, 1:100), $CD4^+$ T cells ($CD4^+$, 1:160), and $CD8^+$ T cells ($CD8^+$, 1:50) were identified using directly conjugated anti-mouse antibodies. In brief, the splenocytes and the serum were blocked with Fc-block (eBioscience) to reduce non-specific antibody binding, and they were incubated in the dark with the appropriate fluorochrome-conjugated antibody for 20 min at 4°C. The cells were then washed with a FACS buffer. The blood was lysed for 5 min with a FACS lysis buffer (BD Bioscience) at room temperature, and re-washed with a FACS buffer. Finally, each sample was fixed with 1% paraformaldehyde until further analysis. Flow cytometry analysis was performed on the FACSCalibur system (BD Biosciences). Control samples were matched for each fluorochrome. Data were analyzed using CellQuest software (Becton Dickinson) (Vendrame et al., 2006).

Gene expression of tissue

Gene expression analysis using RT-PCR was evaluated. For the preparation of total RNA, the RNAgent Total RNA Isolation System (Promega) was used according to the manufacturer's instructions. Amplified cDNA products were separated on 1.5% agarose gel by electrophoresis. Primers used for the respective gene are shown in Table I.

Histopathology

Histopathology analysis was performed and read under the responsibility of pathologist (Biotoxtech). In brief, lungs from each mouse were fixed with 10% neutral buffered formalin and processed using routine histological techniques. After paraffin embedding, 3 mm sections were cut and stained with hematoxylin and eosin (H&E) for histopathological evaluation. Phagocytosis was determined by the dark color of cells, which was read under the responsibility of pathotoxicologist in a GLP facility.

Table I. Primer sequences used in this study

Primer	GB NO.	Sequence
MMP 1a	NM 032006	(L) : gaaggaggccactggtgatt (R) : tcagcccaaataactgctgc
MMP 9	NM 013599	(L) : ggtcttccccaaagacctga (R) : aggcctttgaaggtttggaa
MMP 11	NM 008606	(L) : cccatgccttcttccctaag (R) : gctgtggtgtgttgtagccc
MMP 13	NM 008607	(L) : tggacaagcagttccaaagg (R) : aatggcatcaagggataggg
MMP 15	NM 008609	(L) : atgacatggggcagacacac (R) : ctttgggggttccacagact
MMP 17	NM 011846	(L) : ctatttcttccgaggccagg (R) : aggatgccttggcagagact
MMP 19	NM 021412	(L) : ggccagaactgaccttagcc (R) : gagtaacgtccccggttgat
MMP 23	NM 011985	(L) : tgatggtcccacaggtgaac (R) : cgcctgatcttgctgtgagt
MMP 28	NM 080453	(L) : gatccccactgtcagaggct (R) : ttgtgtctccagcacccagt
Timp 1	NM 011593	(L) : tatgcccacaagtcccagaa (R) : cctgatccgtccacaaacag
SOD 1	NM 011434	(L) : cgtccatcagtatggggaca (R) : aatggacacattggccacac
HSP 1a	NM 010479	(L) : gctggattactgacagcgga (R) : ccgagttcaggatggttgtg
HSP 8	NM 031165	(L) : tcacagtgcccgcttacttc (R) : gcagcagcagttggttcatt

Statistics

Statistically difference was analyzed using one-way ANOVA test. Then, the results obtained from the chemically-treated groups were compared to those of the control group by Student t-test.

RESULTS

Physico-chemical properties of PNPs

We measured the physico-chemical properties of PNPs suspended in PBS prior to the toxicity tests. As

shown in Fig. 1A, PNPs showed quadrangle structure, average particle sizes were 20.9 ± 11.4 nm (Fig. 1B), surface charge was 4.96 ± 3.77 mV, average mobility was 0.39 (μ/s)/(V/cm), and conductance was 24,831 μS.

Decrease of intracellular GSH by PNPs

It is known that cellular antioxidant molecules such as GSH decrease when oxidative stress is increased in the cells. In this study, the intracellular GSH level was decreased after instillation (Fig. 2). The GSH level in the BAL cells of the control group was 10.6 nmol/mg protein. However, the level was down to less than 70% on day 28 after instillation.

Increase of cytokine by PNPs

We measured proinflammatory cytokine (IL-1, TNF-α and IL-6), TH0 cytokine (IL-2), TH1 cytokine (IL-12), TH2 cytokine (IL-4 and IL-5), and tissue damage-related cytokine (TGF β) in the BAL and the blood (Fig. 3 and 4). In the BAL, IL-1, TNF-α, and IL-6 reached their maximum level on day 1 after instillation, and the detection level was 38.0 ± 0.5 pg/mL, 62.1 ± 5.6 pg/mL, and 78.7 ± 4.3 pg/mL, respectively. IL-2 reached its maximum level (12.5 ± 0.4 pg/mL) on day 14, IL-12 was detected at 68.3 ± 5.0 pg/mL on day 1, and IL-4 and IL-5 reached 12.0 ± 0.8 pg/mL and 6.0 ± 0.0 pg/mL on day 14. Furthermore, TGF-β was increased to 18.3 ± 0.0 pg/mL on day 14. In the serum, however, the others were not detected to a significant level, whereas IL-6 and IL-12 reached their maximum level at 49.0 ± 0.3 pg/mL and 159.0 ± 6.4 pg/mL on day 1 and day 14 after instillation, respectively.

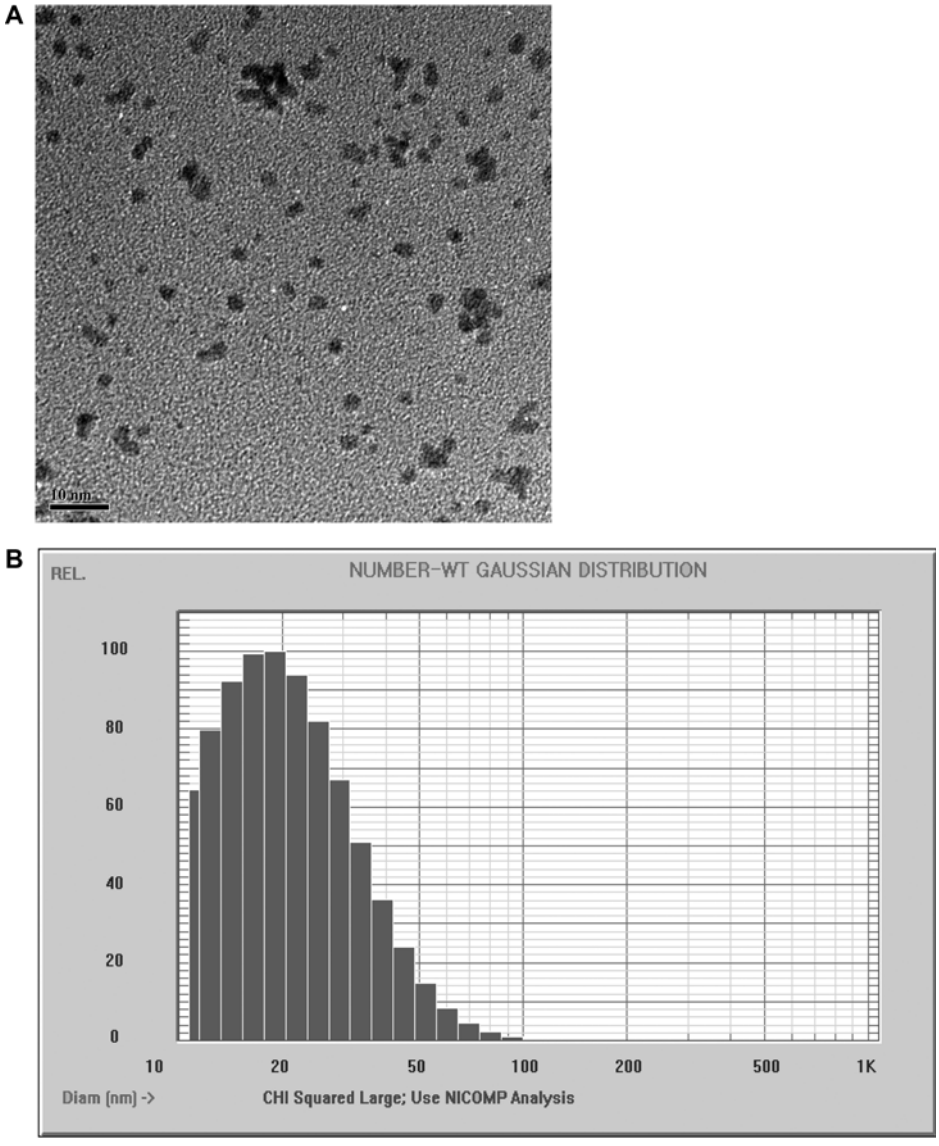

Fig. 1 TEM image and size distribution of PNPs: (**A**) TEM image, (**B**) Size distribution

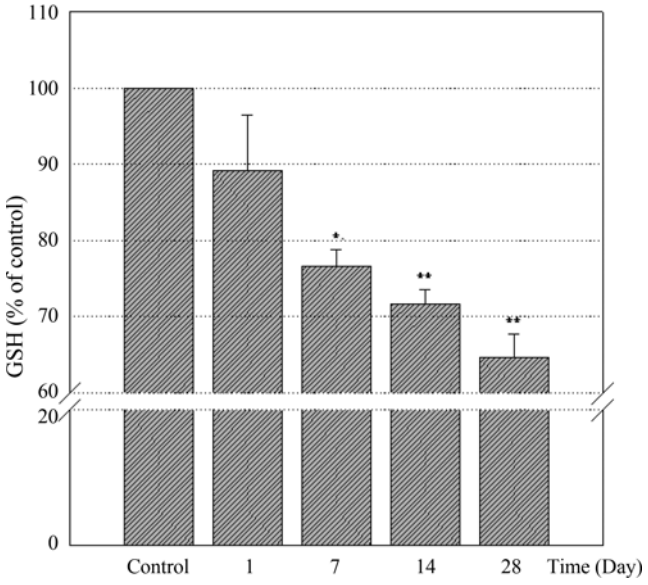

Fig. 2. Decrease of GSH in the total cells of BAL fluid. Mice were treated with PNP (1 mg/kg) by a single intratracheal instillation and they were sacrificed on the designated days. Four mice were pooled to make one test sample from total 12 mice (n = 3). GSH was calculated as nmol of glutathione per mg of protein and then presented as the percentage of the control group. Significantly different from control group, $*p < 0.05$, $**p < 0.01$.

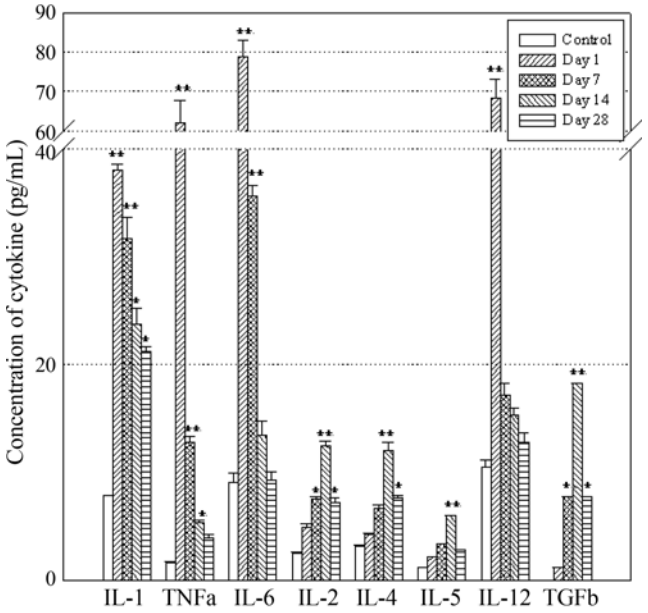

Fig. 3. Changes of cytokine levels in BAL fluid after a single instillation of PNPs. Mice were treated with PNP (1 mg/kg) by a single intratracheal instillation and they were sacrificed on the designated days. Four mice were pooled to make one test sample from total 12 mice (n = 3). Significantly different from control group, $*p < 0.05$, $**p < 0.01$.

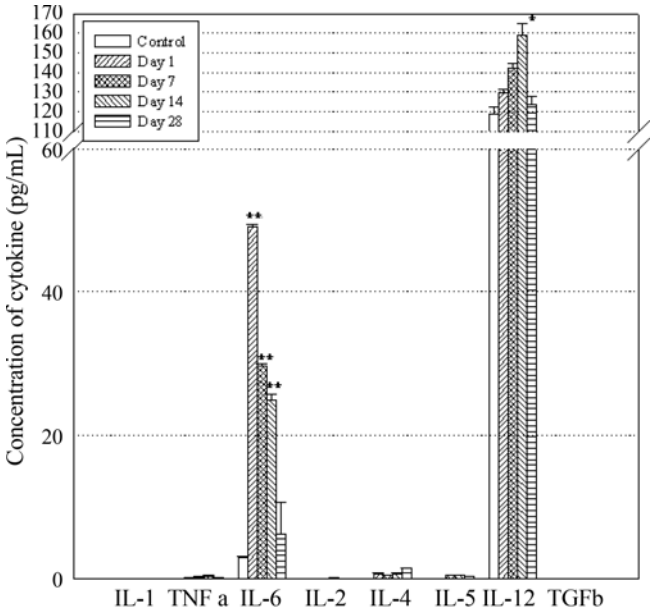

Fig. 4. Changes of cytokine levels in the blood after a single instillation of PNPs. Mice were treated with PNP (1 mg/kg) by a single intratracheal instillation and they were sacrificed on the designated days. Four mice were pooled to make one test sample from total 12 mice (n = 3). Significantly different from control group, $*p < 0.05$, $**p < 0.01$.

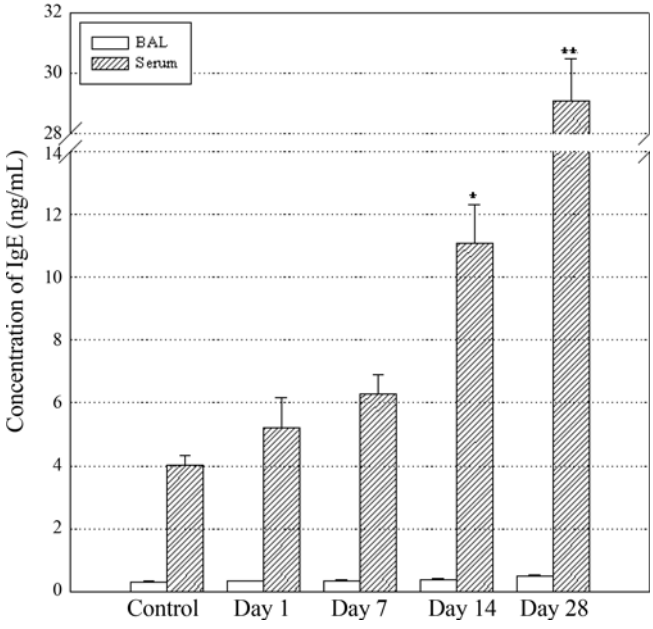

Fig. 5. Levels of IgE in BAL fluid and in blood after a single instillation of PNPs. Mice were treated with PNP (1 mg/kg) by a single intratracheal instillation and they were sacrificed on the designated days. Four mice were pooled to make one test sample from total 12 mice (n = 3). Significantly different from control group, $*p < 0.05$, $**p < 0.01$.

Increase of IgE by PNPs

IgE levels in the BAL fluid and serum were shown in Fig. 5. In the blood, IgE concentration was time-dependently increased, and the detection level was 5.2

± 1.0 ng/mL on day 1, 6.3 ± 0.6 ng/mL on day 7, 11.7 ± 1.2 ng/mL on day 14, and 29.1 ± 1.4 ng/mL on day 28 after instillation. That of control was 4.0 ± 0.3 ng/mL. However, IgE level in BAL fluid was very low when compared with those of serum level and the increased by PNPs was not recognized.

Change of cell phenotype by PNPs

We investigated the changes of cellular distribution in the lymphocytes (Fig. 6). In the blood of the control group, portions of the NK cells, NKT cells, B cells, and T cells were 7.34%, 4.58%, 25.02%, and 63.06%, but cell compositions for the day 28-group changed to 3.28%, 2.20%, 67.48%, and 27.04%, respectively. This result means that the distribution of B cells was increased by PNPs. The changes of cellular distribution shown in blood were also observed in the spleen. We also investigated the composition of the T cell subtypes in the blood. The ratio of $CD4^+$ T cells to $CD8^+$ T cells ($CD4^+/CD8^+$) changed from 3.52 in the control group to 2.91 for the day-28 group, which shows the increase of $CD8^+$ T cells.

Change of gene expression by PNPs

We investigated the changes of gene expression by PNPs. As shown in Fig. 7, the expressions of matrix metalloproteinase (MMP) -9, -11, -13, -17, and -23, and heat shock protein (HSP) 70 family, 1A and 8A

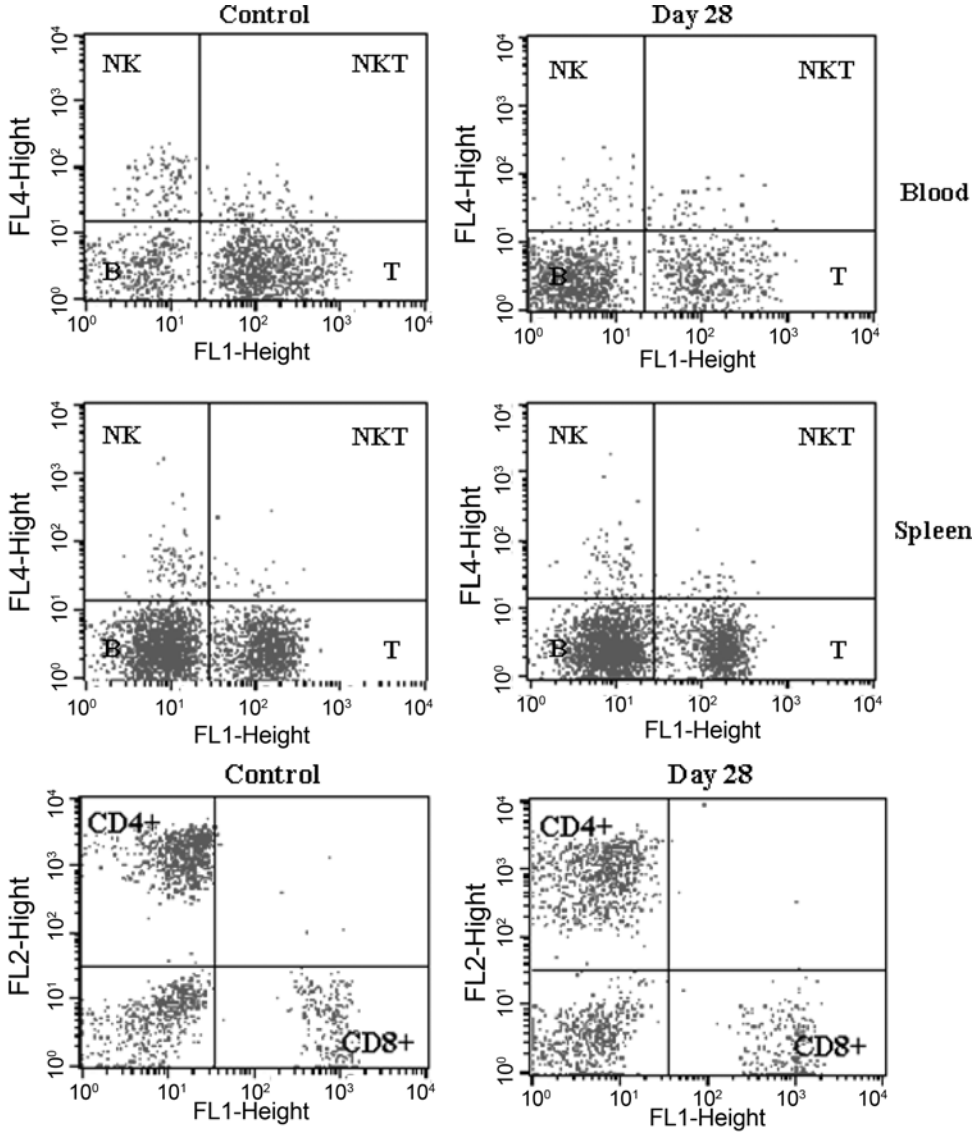

Fig. 6. Analysis of lymphocyte phenotypes by a single instillation of PNPs. Mice were treated with PNPs (1 mg/kg) by a single intratracheal instillation and they were sacrificed on day 28. Four mice were pooled to make one test sample from total 12 mice (n = 3). (**A**) lymphocyte phenotypes in the blood and in the spleen. (**B**) T subtypes in the blood lymphocytes.

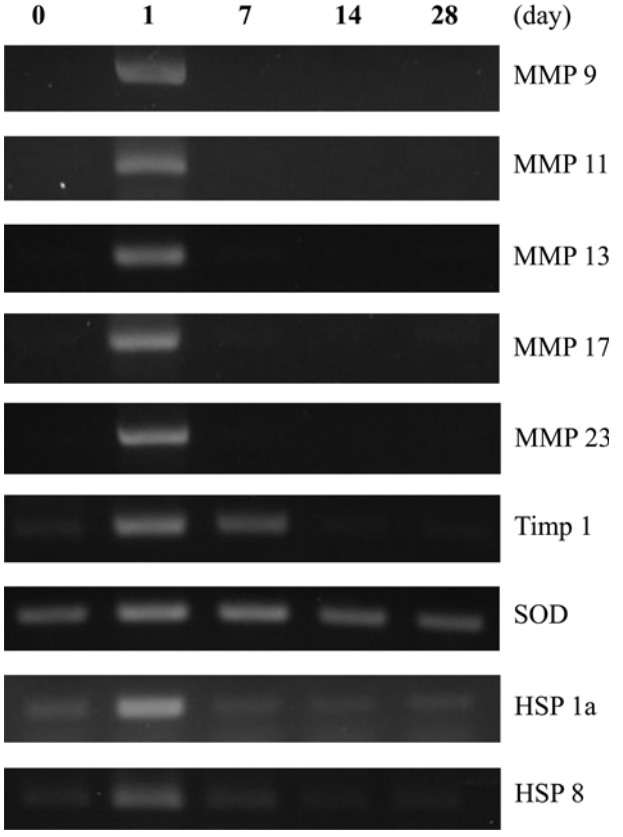

Fig. 7. Change of gene expression by a single instillation of PNPs. RNA was extracted from the lungs of the mice treated with PNPs (1 mg/kg) and amplified by RT-PCR using the respective primers described in Table I. Results were confirmed by several separate experiments and representative images were shown.

were increased on day 1 after instillation. But the increased level was not observed during the rest of experimental period. Gene expression of tissue inhibitor of matrix metalloproteinase (Timp) 1 and super oxide dismutase (SOD) were also increased until day 7 after PNPs instillation.

Histological change by PNPs

In the lungs, phagocytosis by alveolar macrophage was observed during the experimental days. Cell infiltration in the lungs was also observed during the experimental period, while microgranulomatous lesions persisted until day 7 (Fig. 8, Table II).

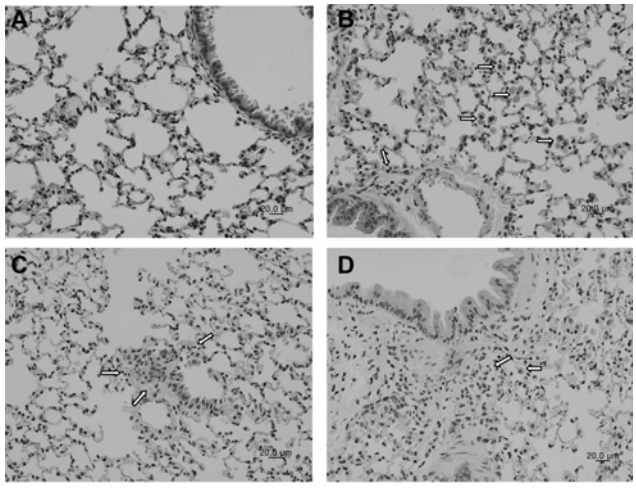

Fig. 8. Histopathology of lung after a single intratracheal instillation of PNPs. Lung sections were stained with hematoxylin and eosin stains (× 200) after a single intratracheal instillation of PNPs (1 mg/kg). (**A**) vehicle control, (**B**) day 1, (**C**) day 14, (**D**) day 28. Arrows indicate cell infiltration.

DISCUSSION

Widespread application of nanoparticles includes enormous potential for human exposure and environmental release. So, the future of nanotechnology will depend on public acceptance of the risk/benefit analysis (Tsuji et al., 2006). In general, manufactured nanoparticles can be produced by top-down and bottom-up methods. Investigation on physico-chemical properties of nanoparticles manufactured by bottom-up methods is essential in determining their potential toxicity in biological systems because the toxicity of nanoparticles mainly depends on their unique physico-chemical properties.

PNPs and gold nanoparticles have been mainly known to have an anti-oxidant and anti-inflammatory effect in biological systems (Tsai et al., 2007; Kim et al., 2008; Larsen et al., 2008; Onizawa et al., 2009). However, some researchers suggested that gold nano-

Table II. Histopathological changes of lung by a single intratracheal instillation of PNPs (1 mg/kg)

	Control	Day 1	Day 7	Day 14	Day 28
Phagocytosis by alveolar macrophage	0	3	1	3	2
Microgranulomatous change around terminal bronchioles	0	1	0	0	0
Cell infiltration (mononuclear cells and macrophage) around alveolar space and alveolar wall	0	2	2	2	2
Cell infiltration (neutrophil) around alveolar space and alveolar wall	0	1	-	1	1

The number of animals which have the respective observation is written. (- : not determined)

particles induce adverse health effects, such as inflammation and oxidative stress *in vivo* and *in vitro* (Goodman et al., 2004; Pan et al., 2007; Tedesco et al., 2008; Cho et al., 2009). It was also reported that PEG-coated gold nanoparticles (13 nm-sized) induced acute inflammation and apoptosis in the liver, and that they were accumulated in the liver and spleen for up to 7 days after injection (Cho et al., 2009). It was also reported that gold nanoparticles (1.4 nm-sized) induced cytotoxicity by oxidative stress, endogenous ROS production, and depletion of the intracellular antioxidant pool (Pan et al., 2007). In our study, PNPs showed time-dependent decrease of intracellular GSH in total cells collected from BAL fluid (Fig. 2). GSH is an important protective antioxidant against free radicals and it has been implicated in immune modulation and inflammatory responses (Rahman and MacNee, 2000; Rahman et al., 2005).

Regulation of proinflammatory cytokines plays an important role in an attack of chronic lung diseases such as allergy, asthma, chronic obstructive pulmonary disease (COPD), and fibrosis (Chung, 2005; Barnes, 2008). IL-1β is produced by macrophages, monocytes, and dendritic cells, and is associated with pain with fever. TNF-α regulates diverse cellular functions such as apoptosis, inflammation, sepsis, and the development of the immune system (Haider and Knöfler, 2009). IL-6 is secreted by T cells and macrophages, and act as chemotactics factor for neutrophils in COPD signaling. In this study, the increased concentrations of pro-inflammatory cytokines in BAL fluid (IL-1, TNF-α, and IL-6) by PNPs treatment were found to be 4.8 fold, 36.5 fold, and 8.7 fold, compared with the level of control group on day 1 after treatment (Fig. 3).

IL-2 contributes to the differentiation and proliferation of T cells activated by macrophage. The concentration of IL-2 increased by 4.9 fold compared to the control group on day 14 after instillation, which reached the highest level. The T cells are differentiated to the TH 1 cells and TH2 cells by TH1-type cytokine (IL-12 and IFN-γ) and TH2-type cytokine (IL-4, IL-5, and IL-10), respectively. However, under many circumstances *in vivo*, there is mixed responses of TH1 and TH2, and the overall effect is determined by which responses dominate. IL-12 rapidly decreased after it increased 6.5 fold for the control group on day 1, while IL-4 and IL-5 remained at a significant level until day 28 after instillation. Furthermore, in this study, TGF-β was remained at a significant level until day 28. The TGF-β inhibits cell proliferation, suppresses immune response, and enhances the formation of extracellular matrix (Lawrence, 1996) (Fig. 3 and Fig. 4).

Previous reports suggested that nanoparticles could be translocated from the lungs to the circulatory system and may induce host responses such as ROS generation, inflammatory cytokine release, and matrix metalloproteinase (MMP) release (Wan et al., 2008). MMPs also play an important role in the destruction of normal tissue architecture, e.g., in rheumatoid arthritis, osteoarthritis, autoimmune blistering skin disorders, cutaneous photoaging, and tumor invasion and metastasis (Johansson et al., 2000). In our study, instillation of PNPs induced the gene expression of MMPs and heat shock protein 70 with formation of microgranuloma in the lung tissue (Fig. 7).

In addition, IgE secretion and distribution of the B cells also markedly increased on day 28 after instillation in this study (Fig. 5 and Fig. 6). According to previous reports, persistent exposure to platinum salt can cause chronic inflammations such as conjunctivitis, urticaria, chronic dermatitis, lacrimation, sneezing, rhinorrhea, coughs, dyspnea, bronchial asthma, and cyanosis. One of these inflammations, bronchial asthma is resulted from both IgE- and cell- mediated immune responses. The induction level of IgE in BAL fluid was very low compared to that of blood.

Based on the results generated in this study, it is suggested that a single intratracheal instillation of PNPs may induce various inflammatory responses with the increases of cytokine production and IgE level.

ACKNOWLEDGEMENTS

This subject was supported by Ministry of Environment as the Eco-technopia 21 project.

REFERENCES

Barnes, P. J., Immunology of asthma and chronic obstructive pulmonary disease. *Nat. Rev. Immunol.*, 8, 183-192 (2008) .

Cheng, H., Xi, C., Meng, X., Hao, Y., Yu, Y., and Zhao, F., Polyethylene glycol-stabilized platinum nanoparticles: the efficient and recyclable catalysts for selective hydrogenation of o-chloronitrobenzene to o-chloroaniline. *J. Colloid Interface Sci.*, 336, 675-678 (2009).

Cho, W. S., Choi, M., Han, B. S., Cho, M., Oh, J., Park, K., Kim, S. J., Kim, S. H., and Jeong, J., Inflammatory mediators induced by intratracheal instillation of ultrafine amorphous silica particles. *Toxicol. Lett.*, 175, 24-33 (2007).

Cho, W. S., Cho, M., Jeong, J., Choi, M., Cho, H. Y., Han, B. S., Kim, S. H., Kim, H. O., Lim, Y. T., Chung, B. H., and Jeong, J., Acute toxicity and pharmacokinetics of 13 nm-sized PEG-coated gold nanoparticles. *Toxicol. Appl. Pharmacol.*, 236, 16-24 (2009).

Chung, K. F., Inflammatory mediators in chronic obstructive pulmonary disease. *Curr. Drug Targets Inflamm. Allergy*, 4, 619-625 (2005).

Gao, J., Liang, G., Cheung, J. S., Pan, Y., Kuang, Y., Zhao, F., Zhang, B., Zhang, X., Wu, E. X., and Xu, B., Multifunctional yolk-shell nanoparticles : A potential MRI contrast and anticancer agent. *J. Am. Chem. Soc.*, 130, 11828-11833 (2008).

Goodman, C. M., McCusker, C. D., Yilmaz, T., and Rotello, V. M., Toxicity of gold nanoparticles functionalized with cationic and anionic side chains. *Bioconjug. Chem.*, 15, 897-900 (2004).

Haider, S. and Knöfler, M., Human tumour necrosis factor: physiological and pathological roles in placenta and endometrium. *Placenta,* 30, 111-123 (2009).

Hamasaki, T., Kashiwagi, T., Imada, T., Nakamichi, N., Aramaki, S., Toh, K., Morisawa, S., Shimakoshi, H., Hisaeda, Y., and Shirahata, S., Kinetic analysis of superoxide anion radical-scavenging and hydroxyl radical-scavenging activities of platinum nanoparticles. *Langmuir,* 24, 7354-7364 (2008).

Johansson, N., Ahonen, M., and Kähäri, V. M., Matrix metalloproteinases in tumor invasion. *Cell. Mol. Life Sci.,* 57, 5-15 (2000).

Kim, J., Takahashi, M., Shimizu, T., Shirasawa, T., Kajita, M., Kanayama, A., and Miyamoto, Y., Effects of a potent antioxidant, platinum nanoparticle, on the lifespan of Caenorhabditis elegans. *Mech. Ageing Dev.,* 129, 322-331 (2008).

Komanicky, V., Iddir, H., Chang, K. C., Menzel, A., Karapetrov, G., Hennessy, D., Zapol, P., and You, H., Shape-dependent activity of platinum array catalyst. *J. Am. Chem. Soc.,* 131, 5732-5733 (2009).

Larsen, A., Kolind, K., Pedersen, D. S., Doering, P., Pedersen, M. O., Danscher, G., Penkowa, M., and Stoltenberg, M., Gold ions bio-released from metallic gold particles reduce inflammation and apoptosis and increase the regenerative responses in focal brain injury. *Histochem. Cell Biol.,* 130, 681-692 (2008).

Lawrence, D. A., Transforming growth factor-beta: a general review. *Eur. Cytokine Netw.,* 7, 363-374 (1996).

Manosroi, A., Saraphanchotiwitthaya, A., and Manosroi, J., *In vitro* immunomodulatory effect of Pouteria cambodiana (Pierre ex Dubard) Baehni extract. *J. Ethnopharmacol.*, 101, 90-94 (2005).

Onizawa, S., Aoshiba, K., Kajita, M., Miyamoto, Y., and Nagai, A., Platinum nanoparticle antioxidants inhibit pulmonary inflammation in mice exposed to cigarette smoke. *Pulm. Pharmacol. Ther.,* 22, 340-349 (2009).

Pan, Y., Neuss, S., Leifert, A., Fischler, M., Wen, F., Simon, U., Schmid, G., Brandau, W., and Jahnen-Dechent, W., Size-dependent cytotoxicity of gold nanoparticles. *Small,* 3, 1941-1949 (2007).

Park, E. J., Choi, J., Park, Y. K., and Park, K., Oxidative stress induced by cerium oxide nanoparticles in cultured BEAS-2B cells. *Toxicology*, 245, 90-100 (2008).

Park, E. J., Yoon, J., Choi, K., Yi, J., and Park, K., Induction of chronic inflammation in mice treated with titanium dioxide nanoparticles by intratracheal instillation. *Toxicology,* 260, 37-46 (2009).

Rahman, I. and MacNee, W., Regulation of redox glutathione levels and gene transcription in lung inflammation : therapeutic approaches. *Free Radic. Biol. Med.,* 28, 1405-1420 (2000).

Rahman, I., Biswas, S. K., Jimenez, L. A., Torres, M., and Forman, H. J., Glutathione, stress responses, and redox signaling in lung inflammation. *Antioxid. Redox Signal.,* 7, 42-59 (2005).

Schmid, M., Zimmermann, S., Krug, H. F., and Sures, B., Influence of platinum, palladium and rhodium as compared with cadmium, nickel and chromium on cell viability and oxidative stress in human bronchial epithelial cells. *Environ. Int.,* 33, 385-390 (2007).

Tedesco, S., Doyle, H., Redmond, G., and Sheehan, D., Gold nanoparticles and oxidative stress in Mytilus edulis. *Mar. Environ. Res.,* 66, 131-133 (2008).

Teranishi, T., Hosoe, M., Tanaka, T., and Miyake, M. B., Size control of monodispersed Pt nanoparticles and their 2D organization by electrophoretic deposition., *J. Phys. Chem. B.,* 103, 3818-3827 (1999).

Theron, A. J., Ramafi, G. J., Feldman, C., Grimmer, H., Visser, S. S., and Anderson, R., Effects of platinum and palladium ions on the production and reactivity of neutrophil-derived reactive oxygen species. *Free Radic. Biol. Med.,* 36, 1408-1417 (2004).

Tsuji, J. S., Maynard, A. D., Howard, P. C., James, J. T., Lam, C. W., Warheit, D. B., and Santamaria, A. B., Research strategies for safety evaluation of nanomaterials, part IV: risk assessment of nanoparticles. *Toxicol. Sci.,* 89, 42-50 (2006).

Tsai, C. Y., Shiau, A. L., Chen, S. Y., Chen, Y. H., Cheng, P. C., Chang, M. Y., Chen, D. H., Chou, C. H., Wang, C. R., and Wu, C. L., Amelioration of collagen-induced arthritis in rats by nanogold. *Arthritis Rheum.,* 56, 544-554 (2007).

Vendrame, M., Gemma, C., Pennypacker, K. R., Bickford, P. C., Davis Sanberg, C., Sanberg, P. R., and Willing, A. E., Cord blood rescues stroke-induced changes in splenocyte phenotype and function. *Exp. Neurol.,* 199, 191-200 (2006).

Wan, R., Mo, Y., Zhang, X., Chien, S., Tollerud, D. J., and Zhang, Q., Matrix metalloproteinase-2 and -9 are induced differently by metal nanoparticles in human monocytes: The role of oxidative stress and protein tyrosine kinase activation. *Toxicol. Appl. Pharmacol.,* 233, 276-285 (2008).

Wang, X., Liu, F., Andavan, G. T., Jing, X., Singh, K., Yazdanpanah, V. R., Bruque, N., Pandey, R. R., Lake, R., Ozkan, M., Wang, K. L., and Ozkan, C. S., Carbon nanotube-DNA nanoarchitectures and electronic functionality. *Small,* 2, 1356-1365 (2006).